

# Mannose-induced Dymorphogenesis of Metanephric Kidney

## Role of Proteoglycans and Adenosine Triphosphate

Zheng Z. Liu, Frank A. Carone, Tomasz M. Dalecki, Brigitte Lelongt, Elisabeth I. Wallner, and Yashpal S. Kanwar  
Department of Pathology, Northwestern University Medical School, Chicago, Illinois 60611

### Abstract

Because various fetal anomalies are seen in diabetic offspring, we examined the effects of sugars on proteoglycans (PGs): extracellular matrix (ECM) macromolecules modulating morphogenesis. 13-d-old mouse metanephric kidney explants were exposed to mannose for 7 d and labeled with [<sup>35</sup>S]sulfate, [<sup>35</sup>S]-methionine, or [<sup>3</sup>H]thymidine. Mannose exposure caused reduction in kidney size and disorganization of ureteric bud branches with inhibition of glomerulogenesis. Tissue autoradiographic and immunofluorescence studies indicated decreased expression of sulfated PGs in ECMs. *Helix pomatia* lectin binding to D-GalNAc residues of glomerular epithelial cells was also reduced. Biochemical studies revealed decreased synthesis of sulfated PGs. PGs were of lower molecular weight with reduced charge density and increased chondroitin/heparan sulfate ratio. Immunoprecipitation of [<sup>35</sup>S]methionine-labeled proteins confirmed the reduction of PG core peptides. Intracellular ATP levels were reduced. The addition of 0.1 mM ATP to culture media restored kidney size, the population of glomeruli, and the synthesis and characteristics of PGs to almost normal, with no detectable effect on the replication of cells as determined by [<sup>3</sup>H]thymidine incorporation. The effect of ATP could be partially blocked by the P<sub>2y</sub>-purinoreceptor, i.e., reactive blue-2. Data suggest that mannose causes energy depletion by cellular ATP consumption and thus selectively alters the synthesis of heavily glycosylated proteins with rapid turnover, such as PGs, resulting in renal dymorphogenesis. (*J. Clin. Invest.* 1992. 90:1205–1218.) Key words: mannose • metanephric kidney • morphogenesis/organogenesis • proteoglycans

### Introduction

Dymorphogenesis of various organ systems has been observed in hyperglycemic states, and these structural defects are two to three times more common in the offsprings of diabetics as compared to the control population (1–4). The diabetic-induced dymorphogenesis commonly affects the heart, skeleton, central nervous system, and kidney, and its severity varies from one organ to another (3). For instance, in the central nervous system there may be a failure in the closure of the neural tube and in the urinary tract there may be renal agenesis (3). Similarly, a higher incidence of morphogenetic defects has been

observed in the offspring of streptozotocin-induced diabetic rats and mice compared to the controls (5–7). These observations suggest that these defects in morphogenesis are not genetically transmitted but are related to environmental factors or the milieu in which the organs are developing. Support for this contention is the experiments in which exposure of rat embryos to elevated concentrations of various sugars resulted in the nonclosure of the neural tube (8). Among the various sugars, mannose induced the most marked and reproducible defects in morphogenesis (9). However, the mechanisms by which hyperglycemic states perturb morphogenesis remain unclear.

In embryonic development, cell adhesion molecules and components of the extracellular matrix (ECM)<sup>1</sup> play a significant role in organogenesis (10–14). There is an extensive literature on cell–matrix interactions and the role of ECM components (type IV collagen, laminin, proteoglycan [PG], etc.) in embryonic development (reviewed in reference 15). With induction of the metanephric mesenchyme by the ureteric bud, coordinated expression of CAMs and ECM components modulate the temporal and spatial structural and functional polarity of renal tubules and glomerulogenesis (15). PGs especially play an apparent key role in organogenesis of various organs including salivary gland, breast, lung, and kidney (16–22).

Our laboratory and others have found a decreased de novo synthesis of PGs in diabetes (23, 24), suggesting that hyperglycemic states perturb the biosynthesis of PGs. This, in turn, could be responsible for various morphogenetic defects observed in hyperglycemic states. This hypothesis was investigated by determining the effect of elevated concentrations of one of the sugars, i.e., D-mannose, on PG biosynthesis and on the morphogenesis of metanephric kidney.

### Methods

An organ culture system was used, and various metanephric differentiation events were investigated by morphological and biochemical techniques under the influence of D-mannose.

*Organ culture system.* Embryonic kidneys were explanted and maintained in an organ culture system as detailed previously (20, 21, 25). Briefly, Swiss-Webster mice (Charles River Breeding Laboratories, Inc., Wilmington, MA) were allowed to mate in pairs in individual cages. At 13 d of gestation, the embryos were harvested aseptically and immersed in a sterilized defined medium consisting of equal volumes of Dulbecco's modified Eagle's medium and Ham's nutrient mixture F12 (Sigma Chemical Co., St. Louis, MO), supplemented with transferrin (50 µg/ml), penicillin (100 µg/ml), and streptomycin (100 µg/ml), and pH maintained at 7.4. Metanephric tissues dissected from the embryos were placed on a 8.0-µm filter (Millipore Corp., Bedford, MA), floated on the defined medium in 35-mm petri dishes, and main-

Address reprint requests to Dr. Kanwar, Department of Pathology, Northwestern University Medical School, 303 East Chicago Avenue, Chicago, IL 60611.

Received for publication 15 January 1992 and in revised form 28 April 1992.

J. Clin. Invest.

© The American Society for Clinical Investigation, Inc.

0021-9738/92/10/1205/14 \$2.00

Volume 90, October 1992, 1205–1218

1. Abbreviations used in this paper: CS, chondroitin sulfate; ECM, extracellular matrix; EM, electron microscopy; GAGs, glycosaminoglycans; HS-PG, heparan sulfate-proteoglycan; LM, light microscopy.

tained at 37°C in a humidified incubator with a mixture of 95% air and 5% CO<sub>2</sub>.

**Experimental design.** Initially, the metanephric explants were exposed to varying concentrations of D-mannose (5–20 mg/ml) and examined on days 1, 4, and 7. 10 mg/ml of mannose was used for subsequent experiments because this concentration induced optimal biochemical alterations without discernible cytotoxicity by light microscopy (LM) and electron microscopy (EM). At each time point, 50–100 embryonic kidneys per variable were processed for routine morphological and immunofluorescent studies with specific antibody probes and lectins, and for various biochemical and biosynthetic studies. An additional 25–50 explants, per time and variable, were used for ATP determinations and for experiments with various purinoceptor antagonists. For biosynthetic studies of PGs, [<sup>35</sup>S]sulfate (New England Nuclear, Boston, MA) was added to the culture medium (0.5 mCi/ml) for a 12-h interval. The tissues were processed for autoradiography and isolation and characterization of PGs. Other radioisotopes used in this study were [<sup>3</sup>H]thymidine (0.025 mCi/ml) to ascertain the distribution of replicating cells during various stages of glomerular development and [<sup>35</sup>S]methionine (0.25 mCi/ml) to determine total protein synthesis and the status of specific glomerular glycoproteins by immunoprecipitation. For the latter studies, labeling time was reduced to 6 h. Both the metanephric tissues and the media were analyzed for alterations in the biosynthesis of PGs.

**Morphological studies.** The metanephric explants were immersion-fixed in Karnovsky's paraformaldehyde-glutaraldehyde fixative and processed for LM and EM (20, 21). For morphometric analysis, flat longitudinal-serial sections (1 μm thick) were prepared from the mid-point of the whole kidney including the ureteric bud and its branches. At various stages of development, the number of glomeruli per unit area of metanephric tissue was determined as previously described (20, 21).

**Immunohistochemical and histochemical studies.** The following antibodies were employed: anti-heparan sulfate-proteoglycan (HS-PG) (26), anti-laminin (27); anti-type IV-collagen (Collaborative Research, Inc., Waltham, MA), and anti-podocalyxin (28). The specificities of these antibodies have been described in respective publications. FITC-conjugated *Helix pomatia* and wheat germ lectins were used to determine the distribution of N-acetylgalactosamine (D-GalNAc) and N-acetylglucosamine [(D-GlyNAc)<sub>2</sub>] + neuraminic acid (NeuNAc) residues of cell surface glycoproteins, respectively. At designated intervals the kidneys were frozen in isopentane and chilled in liquid nitrogen, and 4-μm cryostat sections were prepared, air-dried, and stored at -70°C. Standard procedures were employed for indirect immunofluorescence (20, 21). For lectin staining, the sections were hydrated with PBS (0.01 M, pH 7.4) for 30 min and then incubated with varying dilutions of FITC-conjugated lectins for 30 min at 22°C. The sections were washed twice with PBS and examined with an ultraviolet microscope equipped with epi-illumination.

**Tissue autoradiographic studies.** [<sup>35</sup>S]sulfate-labeled kidneys were processed for autoradiographic studies (20, 21). For LM autoradiography, serial 1-μm sections at the midplane of the kidney with intact ureteric bud and branches were coated with K5 emulsions (Polysciences, Inc., Warrington, PA). For EM autoradiography, 60-nm sections of various stages of glomerular development were coated with L4 emulsion (Polysciences, Inc.). EM autoradiograms were analyzed morphometrically as detailed previously (29, 30). Briefly, 25 glomeruli of the S-shaped body and of the precapillary stage were photographed and printed to a final magnification of 2,500. The cellular and ECM compartments were designated. The relative area of each compartment was determined by the point-counting method and grain counting was performed by the best-fit circle method. Finally, the grain density was calculated by dividing the total number of autoradiographic grains by the total area points.

The metanephric kidneys radiolabeled with [<sup>3</sup>H]thymidine and [<sup>35</sup>S]methionine were processed only for LM autoradiography. At day 4 after [<sup>3</sup>H]thymidine incorporation, glomeruli only in the outer 0.25-mm cortex were enumerated because, in this region of metanephric

explants at this age, there is a preponderance of immature S-shaped glomeruli and therefore a high degree of DNA replicative activity.

**Biochemical studies.** Extraction of radiolabeled PGs from metanephric tissues was carried out as earlier reported (20, 21). Briefly, after removing the culture media, the kidneys were washed thoroughly with cold medium and extracted with 4 M guanidine hydrochloride solution containing a mixture of protease inhibitors. The unextracted residues were pelleted by centrifugation at 10,000 rpm for 15 min at 4°C and the residues were further hydrolyzed with 0.5 M NaOH at 45°C for 3 h. Aliquots of extract and the hydrolysate were applied to a PD-10 column (Sephadex G-25; Pharmacia Inc., Piscataway, NJ) to determine the total incorporated radioactivity. The remaining portions of the extract and hydrolysate were dialyzed against autoclaved ice-cold distilled water containing 1 mM PMSF, aliquoted, lyophilized, and kept at -70°C. The lyophilized extracts were then reconstituted with GuCl and PGs were characterized by Sepharose CL-4B chromatography (Pharmacia Inc.) before and after treatment with chondroitinase-ABC (ICN Biomedicals, Costa Mesa, CA) or heparitinase (Sigma Chemical Co.), as previously described (20, 21). Similarly, the glycosaminoglycans (GAGs) obtained after alkaline hydrolysis of intact PGs were characterized. The molecular weights of the chains were calculated by comparison of  $K_{av}$  values of the elution peaks with the data obtained for chondroitin sulfate (CS) chains by Wasteson (31). The PGs were also characterized by DEAE-Sephacel chromatography (Pharmacia Inc.) using a continuous gradient of 0.1–1.0 M NaCl in 8 M urea solution containing 50 mM sodium acetate and 0.2% 3-[(3-cholamidopropyl)-dimethylammonio]-1-propanesulfonate (CHAPS, Sigma Chemical Co.), pH 6.0 (20, 32).

The media PGs/GAGs were isolated by use of a PD-10 column and the excluded fractions were collected. An aliquot of the excluded fraction was used to determine the incorporated radioactivity and the remainder was dialyzed against autoclaved ice-cold distilled water containing 1 mM PMSF at 4°C, aliquoted, lyophilized, and stored at -70°C. The media PGs/GAGs were characterized as described above.

To determine the effect of D-mannose per se or its phosphorylated products on biosynthesis of PGs, metanephric kidneys were exposed to mannose 6-phosphate at a concentration of 10 mg/ml in the medium. The experiments were also performed with other control sugars, i.e., L-mannose, D-glucose, and mannitol.

**Experiments with ATP.** Since hyperglycemic levels of mannose may deplete cellular energy reserves and consequentially modulate the biosynthesis of PGs, we proceeded to measure the ATP levels in the metanephric tissues levels by the method of Lang and Michael (33). Briefly, after 1–9 h exposure to mannose, metanephric explants were immediately homogenized in ice-cold 0.3 M perchloric acid and placed on ice for 10 min. The homogenate was centrifuged at 5,000 g for 15 min at 4°C, and supernatant was neutralized to pH 7.0, and 100-μl aliquots prepared and stored at -70°C. An individual aliquot was added to 1 ml of reagent mixture (50 μM Tris, pH 8.0, 100 mM glucose, 0.1 mM MgCl<sub>2</sub>, 50 μM NADP<sup>+</sup>, 0.08 μg/ml glucose-6-phosphate), after which fluorometer readings were recorded before and 10 min after the addition of 10 μl of hexokinase (0.1 μg/ml) to the reaction mixture. Finally, the ATP concentration was calculated by comparing the values to a standard curve, and ultimately expressed as nanomoles of ATP per kidney.

In the repletion experiments, 0.1 mM ATP was included in the medium in the presence and in the absence of D-mannose. The levels of ATP were maintained by replacing the media with fresh ATP every 4 h for the entire culture period. In addition, experiments were carried out to block the effect of ATP by various purinoceptor antagonists, i.e., suramin (Miles Inc., West Haven, CT) reactive blue-2 (34) and 8-phenyltheophylline (Sigma Chemical Co.) (35). They were included in the mannose-containing metanephric culture medium 90 s before the addition of 100 μM ATP. The highest concentration of the antagonist used was 100 μM as well, after which the metanephric explants were radiolabeled with [<sup>35</sup>S]sulfate, and the incorporated radioactivity into the PGs' fractions was determined as described above.

**Experiments with [ $^{35}\text{S}$ ]methionine.** The metanephric glycoproteins radiolabeled with [ $^{35}\text{S}$ ]methionine were quantified by immunoprecipitation. The tissues were extracted with 5 M GuCl solution containing a mixture of protease inhibitors and the total incorporated radioactivity was determined as described above. The extracts were dialyzed against distilled water with 1 mM PMSF, aliquoted, and lyophilized. [ $^{35}\text{S}$ ]methionine-labeled glycoproteins were immunoprecipitated utilizing protein-A Sepharose beads and specific antibodies. The radioactivity incorporated in specific cellular (podocalyxin) and ECM proteins (HS-PG, laminin, and type IV collagen) was determined and normalized to a per kidney basis. The immunoprecipitate of anti-HS-PG was also analyzed by SDS-PAGE-agarose gel (1.2% acrylamide + 0.6% agarose) electrophoresis and autoradiographic fluorography. The molecular weights were estimated by comparison with the migratory distance of cartilage specific monomer of CS-PG.

**Experiments with [ $^3\text{H}$ ]thymidine.** The metanephric tissues radiolabeled with [ $^3\text{H}$ ]thymidine were washed twice with cold medium and treated with 5% trichloroacetic acid for 30 min at 90°C. The hydrolysate was cooled and microfuged, and the supernatant was saved. The radioactivity and DNA by the diphenylamine method (36) were determined and the total [ $^3\text{H}$ ]thymidine incorporation was expressed as disintegrations per minute per microgram of DNA.

**Statistics.** Data were expressed as mean  $\pm$  standard deviation and analyzed by Student's *t* test.

## Results

The aim of this investigation was to correlate the modulatory influence of sugars on *de novo* synthesis of PGs with various stages of metanephric development. Data from our preliminary studies suggest that among various sugars mannose maximally affects the development of the metanephric kidney. Therefore, we concentrated our efforts mainly on the alterations induced by mannose.

The developmental stages of glomeruli in metanephric tissues are similar to those observed in neonatal kidney (37, 38), and they include the vesicle, the S-shaped body, and the precapillary glomerulus. The primitive vesicle develops beneath the renal capsule and, with maturation into precapillary stage, migrates deeper into the cortex (19). In an organ culture system, the glomeruli do not get vascularized so the capillary stage is seldom seen. The vesicle stage, however, at day 1 or 4 in culture is difficult to identify since it resembles tubular segments without formed lumens. Further details of the developmental morphology of metanephric kidneys have been described in our previous publications (20, 21). In this study, features are stressed which relate to mannose-induced alterations in PG metabolism and metanephric development.

**General morphological features.** With exposure to mannose, significant alterations were observed at days 1, 4, and 7 in the various stages of glomerular development and in renal organogenesis. Kidney size decreased variably with time, and at the 7th day  $\sim 25\%$  reduction was noted (Fig. 1, *A* vs. *B*). The ureteric bud and its branches were dilated and their ramifications were disorganized.

The number of the glomeruli in S-shape body and precapillary stages per unit area of kidney, i.e., glomerular density, was decreased on day 4 (Table I). A greater decrease was seen in the population density of precapillary stage glomeruli at day 7 and moreover, a few immature S-shaped body stage glomeruli remained in mannose-exposed kidneys. In fact, on day 4, there was a significantly higher density of immature S-shaped glomeruli in the outer 0.25 mm of the renal cortex, presumably

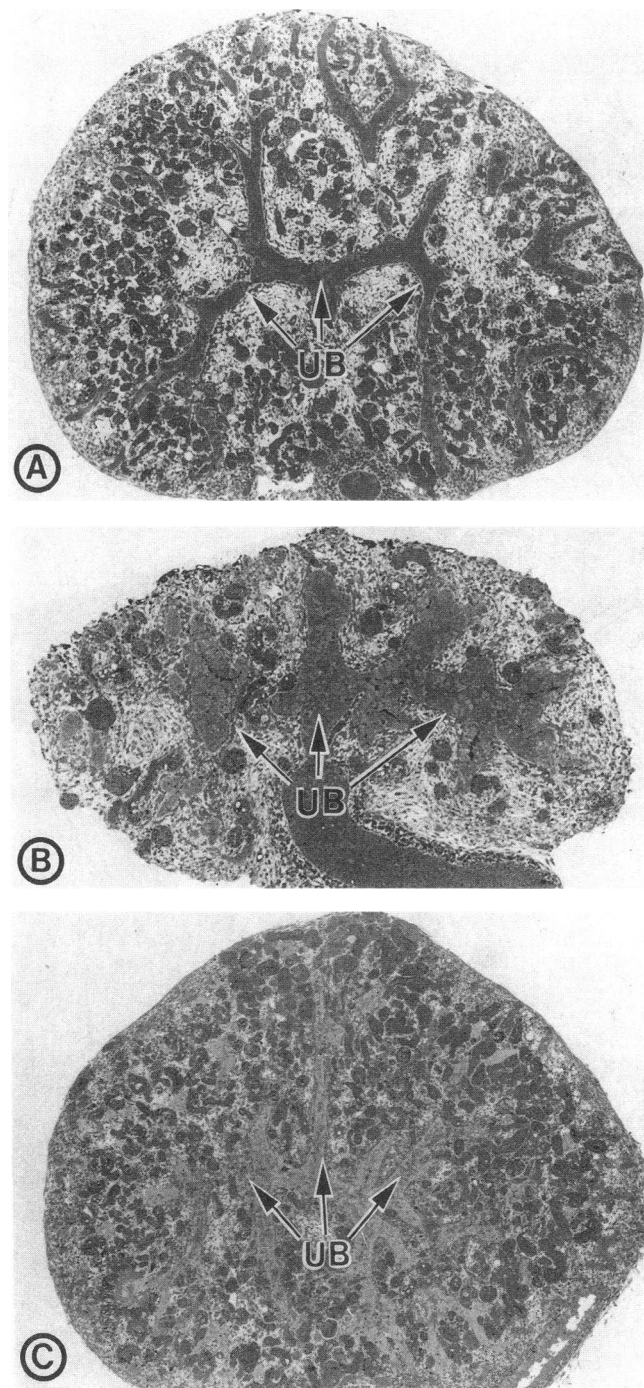


**Figure 1.** Light micrographs of 7-d (*A*) control (*B*) mannose-exposed and (*C*) mannose + ATP-treated embryonic kidneys. The mannose-exposed kidney is smaller and has a reduced population of glomeruli. The ureteric bud (*UB*) branches are dilated and their advancing tips are blunted. With the addition of ATP into the medium (shown in *C*), the kidney size and population of glomeruli reverted to normal.  $\times 30$ .

owing to delayed maturation (Table II). This was further demonstrated by tissue autoradiography of metanephric kidneys labeled with [ $^3\text{H}$ ]thymidine at day 4. The mannose vs. control group had more radioactivity confined to the superficial cortex, whereas in control kidneys autoradiographic grains were seen mainly in the ureteric bud and in its ramifications (Fig. 2,

Table I. Numerical Density of the Glomeruli in the Whole Metanephric Kidney

	S-shaped body	Precapillary
Day 1		
Control	0.23±0.03	
Mannose	0.19±0.02*	
Mannose + ATP	0.22±0.02	
Day 4		
Control	0.07±0.01	0.14±0.02
Mannose	0.06±0.01	0.09±0.01*
Mannose + ATP	0.07±0.02	0.13±0.03
Day 7		
Control		0.25±0.03
Mannose		0.10±0.01*
Mannose + ATP		0.23±0.04

\* Significantly different compared to the control,  $n = 25$ ,  $P < 0.05$ .

*A vs. B*). The total [ $^3\text{H}$ ]thymidine incorporation in the whole kidneys was minimally decreased in the mannose-exposed group as compared to the control ( $30.54 \pm 2.43$  vs.  $34.14 \pm 2.56$  dpm/ $\mu\text{g}$  DNA,  $n = 25$ ).

**Immunohistochemical and histochemical studies.** In the mannose group, a dramatic decrease of intensity of immunofluorescence along the basal lamina of ureteric bud branches, tubules, and the ECM of glomeruli was observed in kidneys stained with anti-HS-PG antibody on day 7 (Fig. 3, *A vs. B*). The metanephric tissues stained with anti-type IV collagen and laminin revealed no appreciable differences in the intensity of fluorescence between the control and mannose group. The anti-podocalyxin antibody revealed immunoreactivity toward glomerular cells, and a mild decrease in the intensity of fluorescence was observed in mannose-exposed kidney. The staining with *Helix pomatia* lectin revealed no differences on day 1 (Fig. 4, *A and B*). However, granular distribution of D-GalNAc residues along the cell surface of glomerular epithelial cells was readily seen in control kidneys by day 7 (Fig. 4 *C*). A mild staining of the ECMs was also observed. In the mannose group, a dramatic decrease of the intensity of fluorescence was observed over the cell surfaces (Fig. 4 *D*). No significant differences were observed in the intensity or distribution of the fluorescence in tissues stained with wheat germ lectin.

**Autoradiographic studies.** Along with the reduction in the population of glomeruli and dysmorphogenesis of the ureteric bud branches in mannose-exposed metanephric tissues, there was a dramatic diminution in the [ $^{35}\text{S}$ ]sulfate incorporation, as

Table II. Number of Glomeruli in S-shaped Body Stage in the Superficial Cortex of the Metanephric Kidney\*

	Day 1	Day 4
Control	14.50±1.49	3.30±0.94
Mannose	12.30±1.48	5.90±1.37†
Mannose + ATP	13.95±1.51	3.27±0.81

\* The superficial cortex included 0.25-mm rim underneath the renal capsule. †  $P < 0.05$  compared to the control,  $n = 25$ .

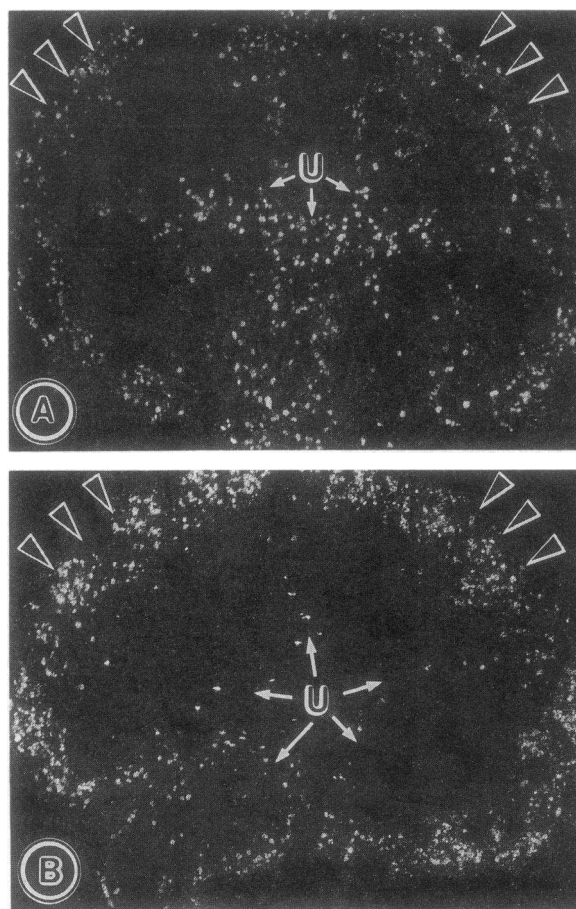
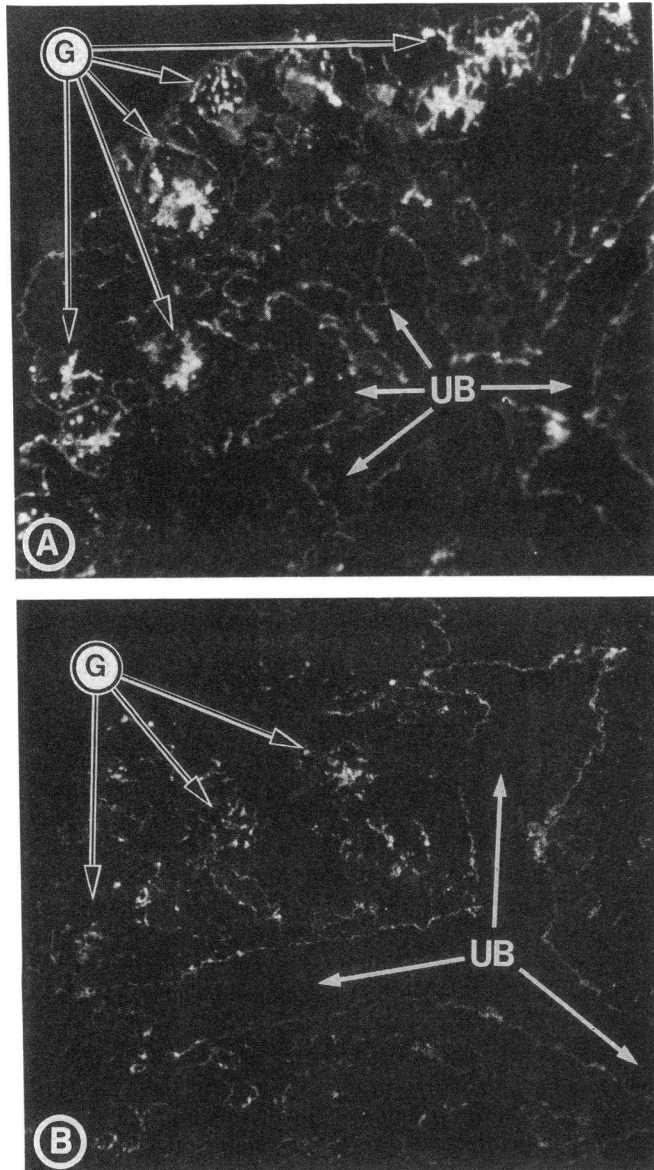


Figure 2. Dark field light microscopic autoradiograms of (A) control and (B) mannose-exposed embryonic kidneys radiolabeled with [ $^3\text{H}$ ]thymidine after 4 d in culture. In control, the radioactivity is seen in the outer 0.25-mm cortex and over the ureteric bud branches (U), whereas in the mannose group, the radioactivity is increased in the cortex and decreased in the ureteric bud branches. The arrowheads outline the boundaries of metanephric kidneys.  $\times 30$ .

reflected by a decrease in grains in LM autoradiograms. A generalized decrease in the autoradiographic grains was seen on day 1, but on day 7, there was a markedly decreased number of grains over the dilated ureteric bud branches, the ECMs of the sparsely distributed glomeruli and the advancing tips of ureteric bud branches (Fig. 5, *A vs. B*).

No distinct morphological changes were observed in the glomeruli on day 1 in the mannose group; however, on day 7, the persistence of S-shaped body stage in the metanephric tissue suggested that mannose had induced a delay in maturation of the glomeruli. In general, the glomeruli were enlarged and the usual organoid appearance of the S-shaped body was not seen in that the cells comprising the tail ends were reduced. The notable alterations in glomerular visceral epithelial cells in precapillary stage included: an increased nuclear/cytoplasmic ratio with prominent nucleoli (Fig. 6, *A vs. B*) and a decrease in cell surface microvilli (see inset of Fig. 6 *A vs. B*). Nuclear changes were also seen in the cells of the S-shaped body glomeruli. No appreciable differences were observed in the Golgi complex, intercellular junctions, and intracellular organelles (Fig. 7, *A vs. B*). However, the visceral epithelial cell foot processes, flanking either side of the glomerular basement



**Figure 3.** Indirect immunofluorescence micrographs of 7-d (A) control and (B) mannose-exposed embryonic kidneys stained with anti-HS-PG. In the mannose group, a decrease in the intensity of fluorescence is seen in the extracellular matrices lining the ureteric bud branches (UB) and precapillary glomeruli (G).  $\times 250$ .

membrane (GBM), were either effaced or poorly developed (see inset of Fig. 7 A vs. that of B). The ECMs were greatly diminished and the glomerular basement membranes were relatively thinner. The parietal epithelial cells of the glomeruli were reduced in number and had an increased nuclear/cytoplasmic ratio.

In kidneys exposed to mannose, autoradiographic studies revealed a decrease of grain densities in both cellular and ECM compartments, especially in the latter (Table III). In the S-shaped body stage at day 1, minimal change in the grain density (concentration of radiation) was observed over the intracellular compartment. Normally, at this stage, most of radioactivity is associated with developing ECMs in the cleft region as we reported previously (19). Mannose induced a significant decrease in the grain density in the extracellular compartment

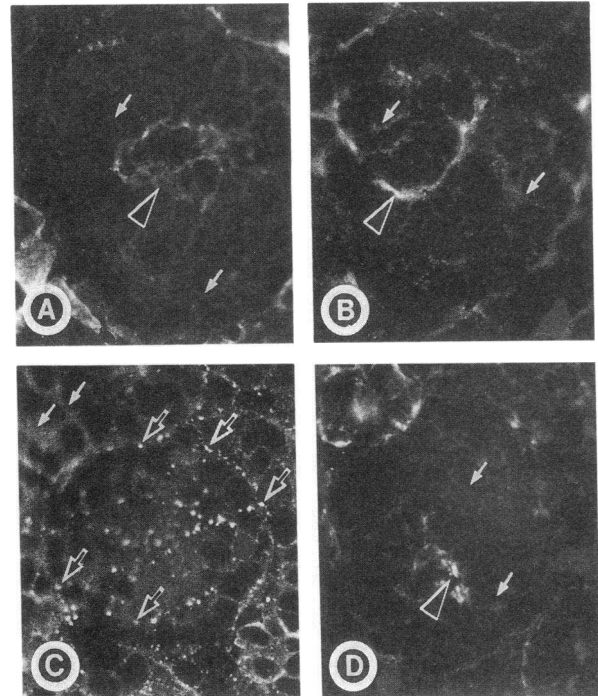


**Figure 4.** Fluorescence micrographs of (A and C) control and (B and D) mannose-exposed embryonic kidneys after (A and B) 1 and (C and D) 7 d in culture and stained with fluoresceinated *Helix pomatia* lectin to detect the presence of D-GalNac residues. (A and B) On day 1 the glomeruli in the S-shaped body stage reveal linear staining of the cell surfaces (white arrows) and the extracellular matrices (arrowheads). (C) On day 7, the glomeruli in precapillary stage show mostly a granular pattern of staining (black and white arrows), indicative of the development of visceral epithelial foot processes. (D) The granular pattern of staining is dramatically reduced in the mannose group, indicative of poor development of the foot processes.  $\times 800$ .

including the cleft region of the S-shaped body and was pronounced on day 4. On day 7 in the precapillary stage, there was a significant drop in the grain density in the intracellular compartment and especially the extracellular compartment, including the GBM (Table III, insets of Fig. 7, A and B). In addition, there appeared to be a slight decrease in the autoradiographic grains associated with Golgi complexes. The concentration of autoradiographic grains over the Bowman's capsular basement membranes and surrounding mesenchyme was comparable to controls (Fig. 6, A vs. B).

**Biochemical studies.** To explore the mechanism(s) for mannose-induced alterations in metanephric development, we investigated the biosynthetic status of various ECM glycoproteins, especially PGs, which are known to modulate organ morphogenesis.

With 98.4% efficiency of extraction, D-mannose induced a dose-dependent decrease in the total incorporated [ $^{35}$ S]sulfate radioactivity (Fig. 8), and the reduced incorporation was seen on days 1, 4, and 7 both in kidney and media (Fig. 9) fractions. Maximal decrease in the incorporation occurred on day 4 in the kidney fraction, and on day 7 in the media fraction. About 95% of the extracted [ $^{35}$ S]sulfate-associated radioactivity was confined to the PG fraction.

PGs in metanephric kidney were characterized by Sephadex CL-4B chromatography. As shown in Fig. 10 A, on day 1,

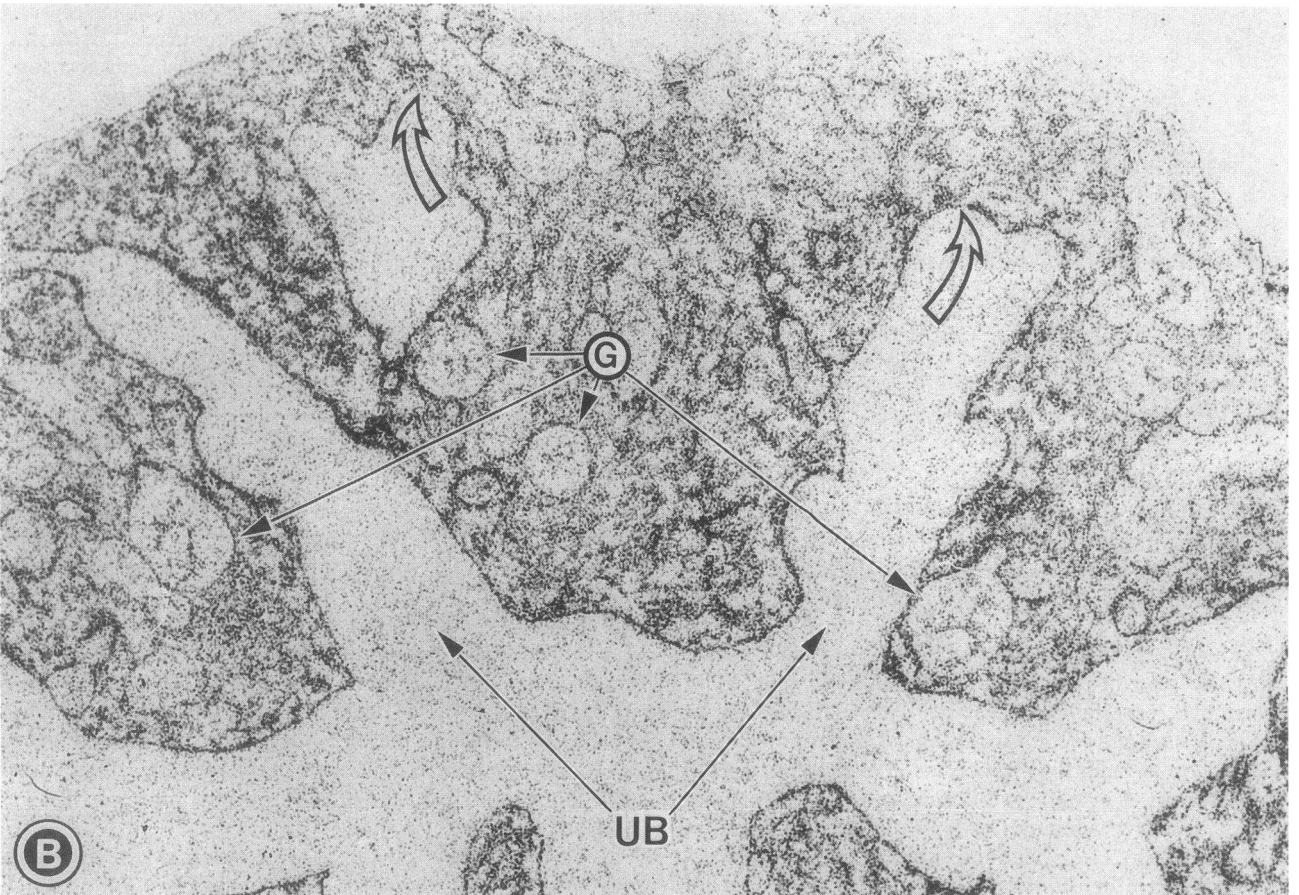
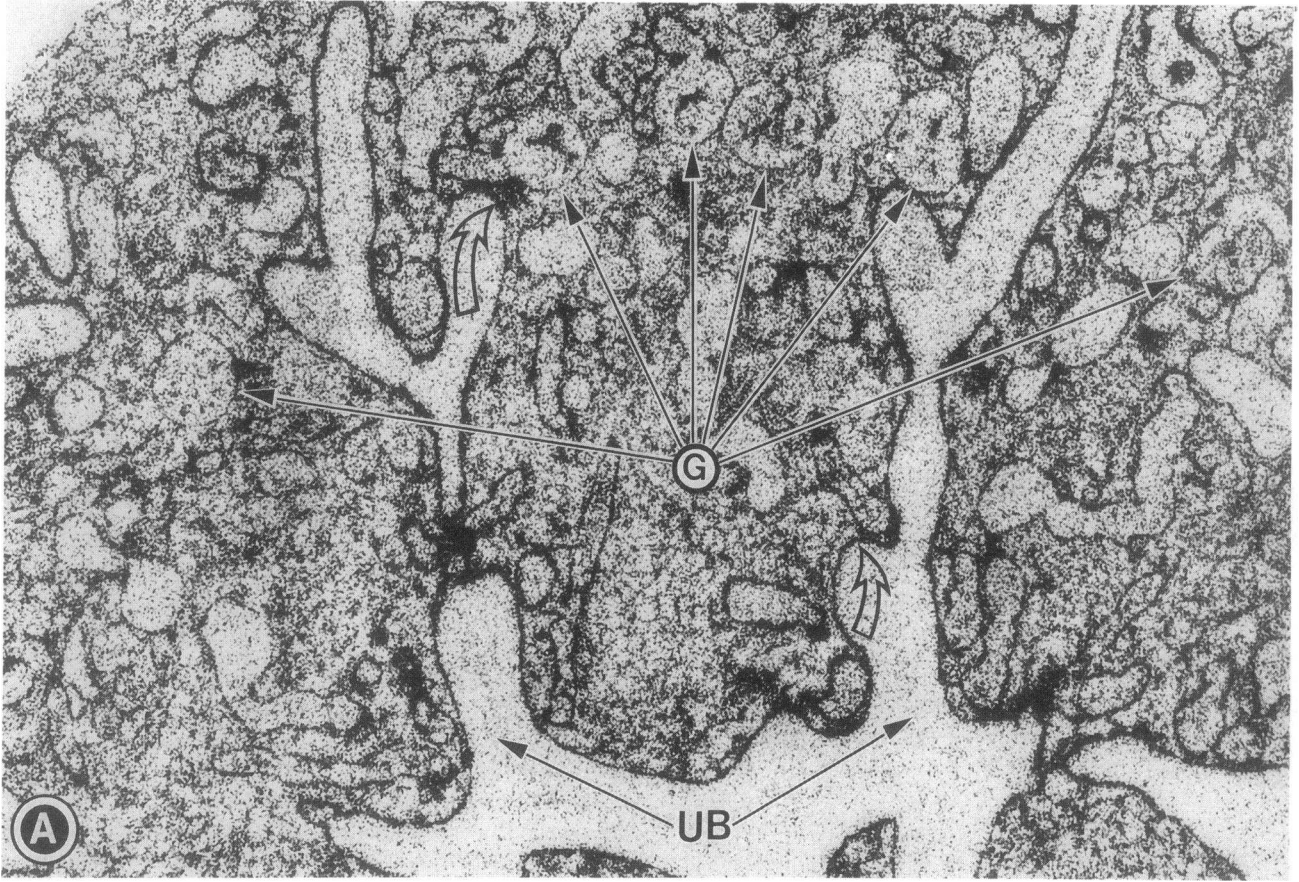


Table III. Autoradiographic Grain Densities of Cellular and Extracellular Compartments in the Various Stages of Glomeruli in Metanephric Tissues

	Control		Mannose	
	Cellular	Extracellular	Cellular	Extracellular
Day 1				
S-shaped body	0.54±0.11	5.01±0.74	0.51±0.19	3.31±0.93*
Day 4				
S-shaped body	0.56±0.13	3.83±0.56	0.54±0.16	2.61±0.87*
Precapillary	0.78±0.17	4.92±0.67	0.58±0.21*	3.70±0.35
Day 7				
Precapillary	0.56±0.12	5.16±0.35	0.27±0.09*	2.81±0.38*

\* Significantly different from control ( $P < 0.01$ ),  $n = 25$ .

in the control group, a major peak (peak *A*) with  $K_{av} = 0.027$  ( $M_r 2.5-3.0 \times 10^6$ ) and two minor peaks (peaks *B* and *C*) with  $K_{av} = 0.38$  ( $M_r \sim 4.0 \times 10^5$ ) and  $0.70$  ( $M_r \sim 3.0 \times 10^4$ ) were observed. The peaks *A* and *B* contained large- and a small-size PGs while peak *C* contained GAG chains only. Treatment with chondroitinase-ABC released  $\sim 30\%$ ,  $\sim 50\%$ , and  $\sim 50\%$  of the radioactivities into the Vt fraction from peaks *A*, *B*, and *C*, respectively. Successive treatments with chondroitinase-ABC (specifically degrades chondroitin A, B, and C sulfates) and heparitinase (specifically degrades heparan sulfate) released all the radioactivities associated with the three peaks into the Vt fraction. On day 1 in the mannose group, elution profiles of PGs/GAGs had  $K_{av}$  values similar to those of controls, however there was a decrease in the radioactivities eluted in peaks *A*, *B*, and *C*.

As shown in Fig. 10 *B*, on days 4 and 7, in control groups, the relative proportions of incorporated radioactivities in peaks *B* and *C* increased. In the mannose group, the tissue PGs also eluted as three peaks with a decrease in the incorporated radioactivity associated with peak *A*. The  $K_{av}$  of all the three peaks shifted to somewhat higher values (Fig. 10 *B*), indicating the synthesis of relatively smaller PGs after the prolonged exposure to mannose. Also, the proportion of de novo synthesized chondroitin/dermatan sulfate increased significantly with increasing exposure to mannose. By day 7, the de novo synthesized PGs contained equal proportions of heparan and chondroitin/dermatan sulfate.

The characterization of tissue GAGs by Sepharose CL-4B or CL-6B chromatographies also revealed a relative increase in the proportion of CS; while the chain size remained the same. Estimated  $K_{av}$  values by Sepharose CL-4B and 6B were 0.69 and 0.42, respectively, with a molecular weight of  $\sim 4 \times 10^3$  (figure not included).

As shown in Fig. 11 *A*, on day 1, the media PGs of controls and mannose groups characterized by Sepharose CL-4B chromatography, revealed two similar peaks, i.e., a predominant peak *A* with  $K_{av} = 0.07$  and a smaller peak *B* with  $K_{av} = 0.55$ . However, a moderate increase in the chondroitinase-ABC sen-

sitive PGs was observed in both the peaks in the mannose-exposed kidneys (figure not included). On day 7, in the control group, two peaks, i.e., a relatively smaller peak *A* with  $K_{av} = 0.18$  and a major peak *B* with  $K_{av} = 0.55$  were observed (Fig. 11 *B*). A slight increase in the CS was observed in both the peaks when compared to day 1. In the experimental group at day 7, the elution peaks shifted to higher  $K_{av}$  values, i.e., peak *A* = 0.31 and peak *B* = 0.60 (Fig. 11 *B*). Both the peaks had relatively higher proportions of chondroitinase-ABC sensitive PGs as compared to control on day 7.

Further characteristics of tissue and media PGs/GAGs were carried out by DEAE-Sephacel chromatography. On day 1 or day 7 there were no differences between the control and experimental groups in the elution profiles of tissue fractions. On day 1, the media PGs/GAGs of control and mannose groups had similar elution patterns (Fig. 12 *A*); however, at day 7, the media PGs/GAGs of the mannose group vs. control eluted at a relatively lower salt concentration (0.40–0.55 vs. 0.35–0.50 M, Fig. 12 *B*), indicating a reduced sulfation of GAG chains.

Attempts were made to characterize tissue and media PGs by SDS-PAGE electrophoresis. On a 5% slab gel, a diffuse smear of radioactivity extending from the point of application to near the bottom of the gel ( $M_r \sim 3 \times 10^4$ ) was seen. Thus, by this method the three peaks (peaks *A*, *B*, and *C*) observed by Sepharose CL-4B chromatography (Fig. 10) could not be resolved.

*Experiments with [<sup>35</sup>S]methionine.* A minor decrease in the [<sup>35</sup>S]methionine incorporation was observed in metanephric tissues exposed to mannose for 4 d ( $2.36 \pm 0.19 \times 10^7$  vs.  $2.20 \pm 0.15 \times 10^7$  dpm/kidney,  $n = 25$ ). No significant differences in the [<sup>35</sup>S]methionine incorporation were observed by tissue autoradiography. Immunoprecipitation with specific antibodies revealed a dramatic reduction, i.e.,  $\sim 3.5$ -fold, in the radioincorporation of [<sup>35</sup>S]methionine into de novo synthesized core-peptide of the PG (Fig. 13). However, immunoprecipitation with anti-laminin, anti-type IV collagen and anti-podocalyxin showed only mild decreases in the radioactivities

Figure 5. LM autoradiograms of 7-d (*A*) control and (*B*) mannose-exposed embryonic kidneys labeled with [<sup>35</sup>S]sulfate. In the mannose group, a dramatic reduction in the radioactivity is observed over the ureteric bud branches (*UB*), on their advancing tips (*open arrows*) and in the precapillary stage glomeruli (*G*).  $\times 200$ .

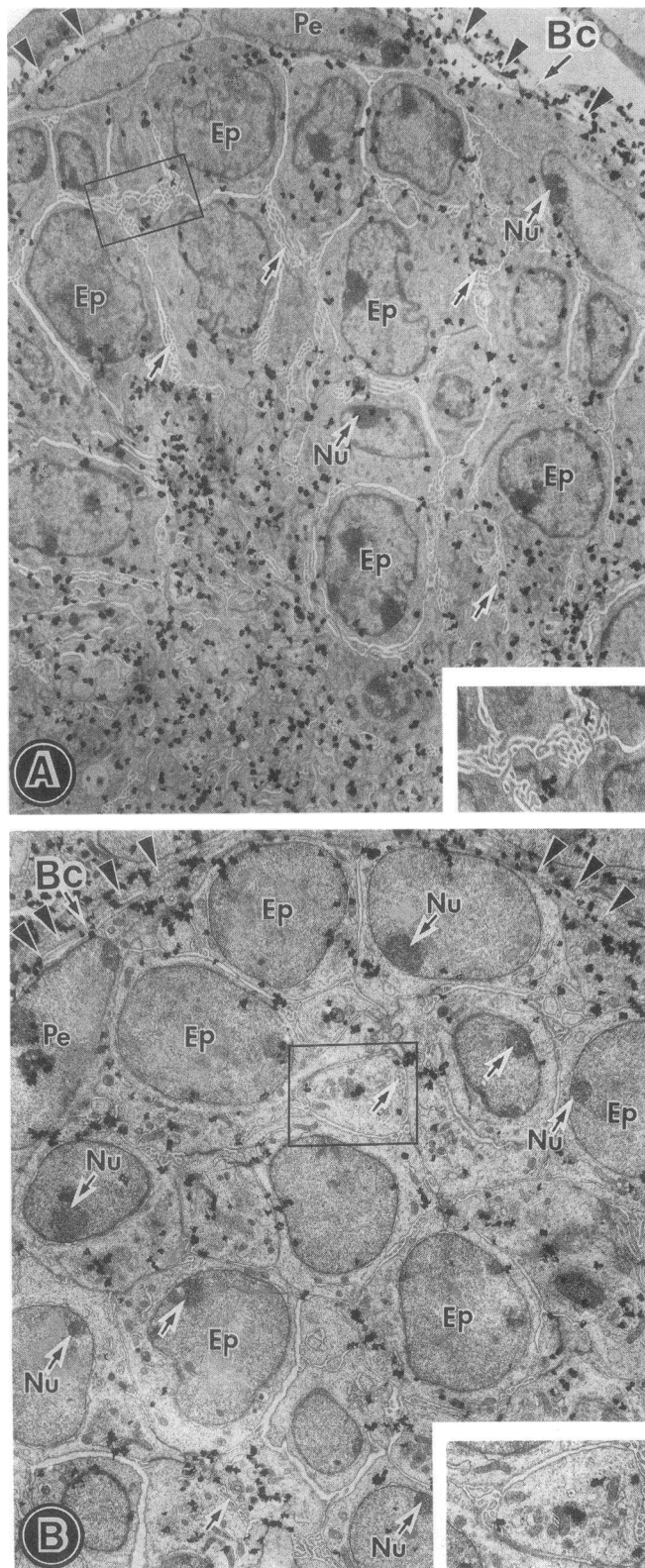


**Figure 6.** EM autoradiograms of precapillary of 7-d (A) control and (B) mannose-exposed kidneys labeled with [<sup>35</sup>S]sulfate. In the mannose group, there is a reduction in the autoradiographic grains, especially in the central region of the precapillary where ECMs are developing and a reduction in the population of cell surface associated villi (arrows and insets). The nuclei of epithelial cells (Ep) are large and have prominent nucleoli (Nu). The concentration of autoradiographic grains (arrowheads) over Bowman's capsule (Bc) are similar to that of the control.  $\times 2,500$ ; (insets)  $\times 5,000$ .

associated with the respective glycoproteins (Fig. 13). SDS-PAGE-agarose gel electrophoresis and autoradiographic fluorography revealed that anti-PG immunoprecipitated radioactivity migrated as a single band which comigrated with PGs radiolabeled with [<sup>35</sup>S]sulfate (Fig. 14, lanes A and C). Also, a dramatic decrease in the radioactivity associated with these bands was observed in the mannose group (Fig. 14, lane B). Most likely, this band corresponds to the [<sup>35</sup>S]sulfate associated radioactivity included in peak A of Sepharose CL-4B chromatograms (Fig. 10) since it migrated at a higher position than that of the cartilage specific chondroitin sulfate-proteoglycan standard ( $M_r \sim 2.6 \times 10^6$ ). However, radioactivity corresponding to peaks B and C (Fig. 10), which included relatively lower molecular weight PGs, were not seen as bands on PAGE-agarose gels.

**Experiments with other sugars.** The exposure of metanephric kidneys to mannose 6-phosphate (10 mg/ml), also decreased [<sup>35</sup>S]sulfate incorporation to the same degree as mannose at the comparable concentration (Fig. 15). The kidney size and glomerular population were also qualitatively reduced. D-Glucose also inhibited the de novo synthesis of sulfated-PGs but to a lesser degree. L-Mannose and mannitol, at comparable concentrations, did not affect [<sup>35</sup>S]sulfate incorporation (Fig. 15) or change in the characteristics of de novo synthesized PGs. Similarly, no change in the size or in the population of glomeruli was observed.

**Experiments with ATP.** Incubation of metanephric kidneys with mannose resulted in a progressive depletion of cellular ATP with time. Within 6 h, the cellular ATP levels were reduced by  $\sim 55\%$  from the basal values, and thereafter the levels did not decrease significantly (Fig. 16). Addition of 100  $\mu$ M ATP into the medium containing mannose (10 mg/ml) restored the de novo synthesis of sulfated PGs by about 90% (Fig. 15) and the characteristics of PGs were similar to those of the control. The kidney size (Fig. 1) and glomerular population reverted to normal (Tables I and II). The total [<sup>3</sup>H]thymidine incorporation was not significantly different from the control ( $33.93 \pm 2.92$  vs.  $34.14 \pm 2.56$  dpm/ $\mu$ g DNA,  $n = 25$ ). Tissue autoradiograms prepared from limited number of metanephric kidneys revealed no qualitative differences from the control. Inclusion of ATP per se did not cause any increase in the de novo synthesis of PGs as compared with the basal control values.

The experiments with purinoceptor antagonists 8-phenyltheophylline ( $P_1$ ) and suramin ( $P_{2x}$ ) revealed no decrease in the incorporation of [<sup>35</sup>S]sulfate into the PGs' fraction in presence of mannose + ATP (Fig. 17). However, reactive blue-2 ( $P_{2y}$ , receptor antagonist) caused maximal  $\sim 30\%$  reduction in the de novo synthesis of sulfated PGs at equimolar concentration of ATP, i.e., 100  $\mu$ M (Fig. 17). This suggests a partial blockage of the effect related to ATP on the biosynthesis of PGs.

## Discussion

The results of this investigation establish a correlation between D-mannose-induced morphologic alterations in the embryonic kidney and changes in the de novo synthesis of PGs during various stages of metanephric culture. At day 1, a decrease in the population of glomeruli was probably secondary to the blunting and disarray of the advancing tips of the ureteric bud

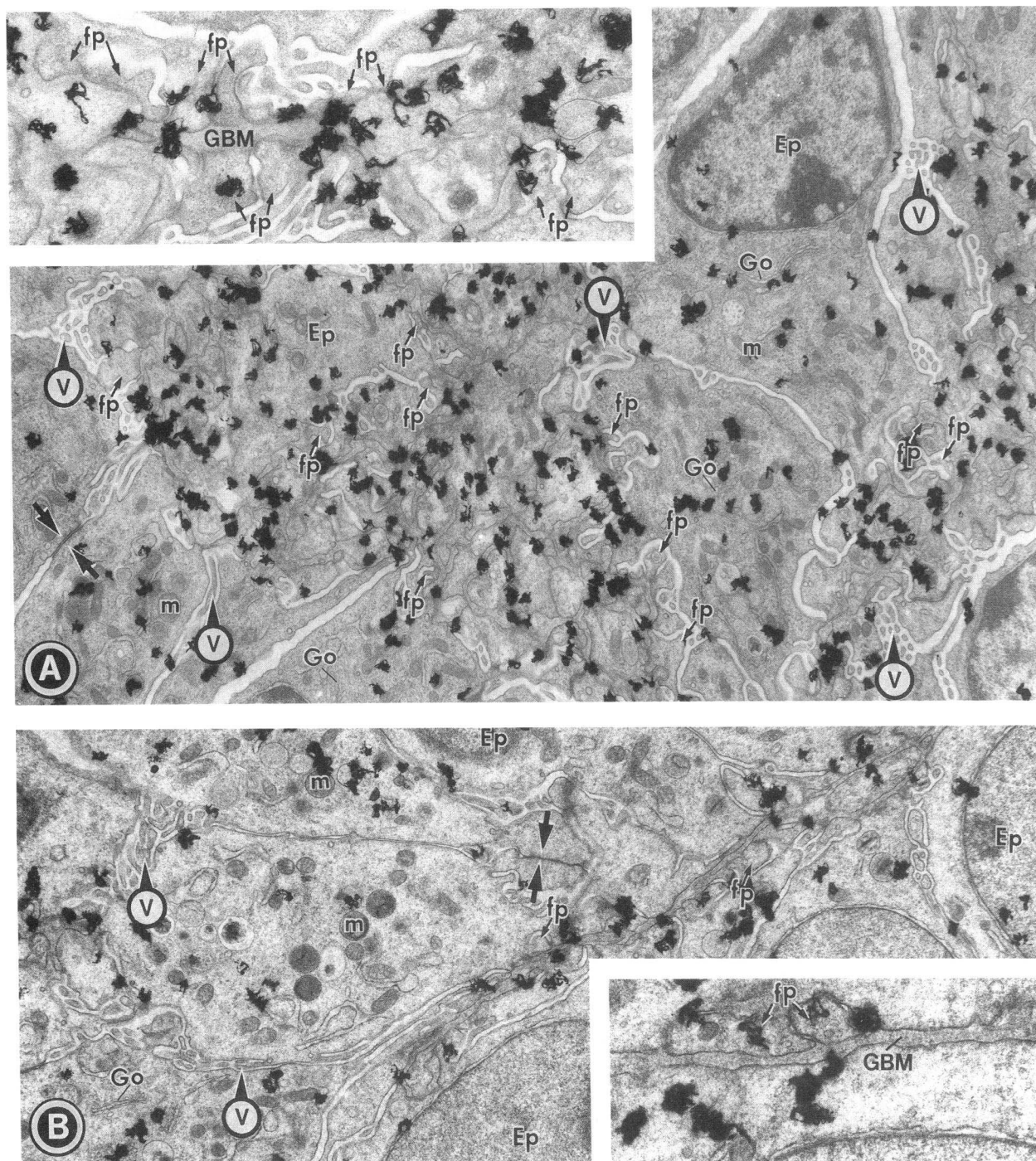


**Figure 7.** EM autoradiograms of precapillary of 7-d (A) control and (B) mannose-exposed kidneys labeled with [ $^{35}$ S]sulfate. In the mannose group, there is a decreased number of autoradiographic grains over both the epithelial cells (*Ep*) and the relatively thinner glomerular basement membrane (*GBM*, insets). The foot processes (*fp*) of epithelial cells are decreased in number and poorly developed. The cell surface villi (*V*) are reduced in number. There are relatively fewer autoradiographic grains associated with intact Golgi saccules (*Go*). The intercellular junctions (opposing arrows) are intact. The mitochondria (*m*) appeared normal.  $\times 10,000$ ; (insets)  $\times 25,000$ .

branches—the region where cell–cell interactions and induction of nephron development occurs (38). A reflection of these defective interactions was the reduction of autoradiographic grains (concentration of radioactivity) over the advancing tips of the ureteric bud branches (Fig. 5). The autoradiographic density was also reduced over glomerular compartments in both the S-shaped body and precapillary stages throughout the culture period. However, the autoradiographic density was dra-

matically reduced on day 4 in the extracellular matrix compartment, especially in the S-shaped body glomeruli (Table III). During this stage, maximal epithelial–mesenchymal interactions take place in the cleft region of the S-shaped body which contains high concentration of PGs (19–21) that modulate morphogenesis. During salivary gland morphogenesis a higher expression of PGs occurs in the cleft region compared to the advancing tips of peripheral lobules and plays a key role in

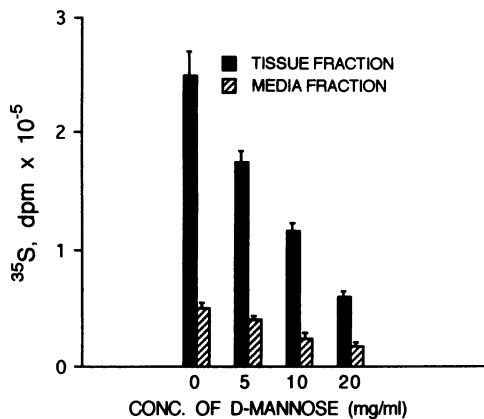


Figure 8. Influence of increasing concentrations of mannose on [<sup>35</sup>S]-sulfate incorporation in metanephric kidney and the release of radio-labeled PGs into the culture media. The tissue and media values were normalized to per unit kidney ( $n = 25$ ).

lobulogenesis (16). Abolition of the differential expression leads to a failure in lobulogenesis. In an analogous manner, interference in the biosynthesis of the PGs in the cleft region could account for poor glomerular development (20, 21). The reduced radioactivity indicative of impaired biosynthesis of PGs in the extracellular compartment, on both days 1 and 4 of mannose exposure, apparently delayed maturation of glomeruli from the S-shaped body to the precapillary stage. This maturational arrest was further reflected by [<sup>3</sup>H]thymidine incorporation on day 4 when minimal DNA-replicative activity was observed in the superficial cortex of controls, in that most glomeruli had already matured from an S-shaped body into the precapillary stage. However, with mannose exposure, a high level of [<sup>3</sup>H]thymidine incorporation in the outer superficial cortex (Fig. 2) was associated with the persistence of glomeruli in the S-shaped body stage (Table II). Thus, the decrease in the nephron population was probably due to (a) an initial failure of glomerulogenesis at the advancing tips of the ureteric bud branches and (b) the arrested maturation of glomeruli later at the S-shaped body stage. Tissue autoradiographic and biochem-

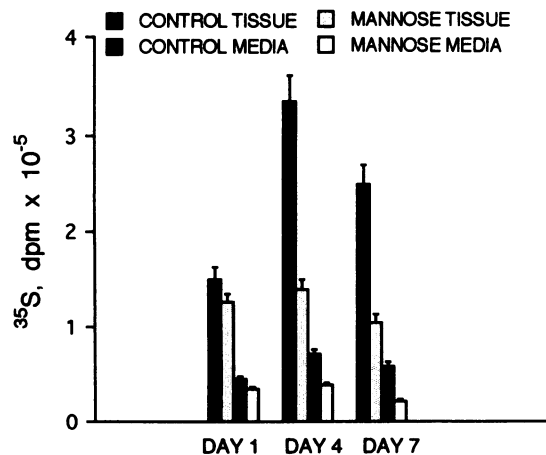


Figure 9. Influence of mannose (10 mg/ml) on [<sup>35</sup>S]-sulfate incorporation into kidney tissue and media fractions as a function of time. The tissue and media values were normalized to per unit kidney ( $n = 25$ ).

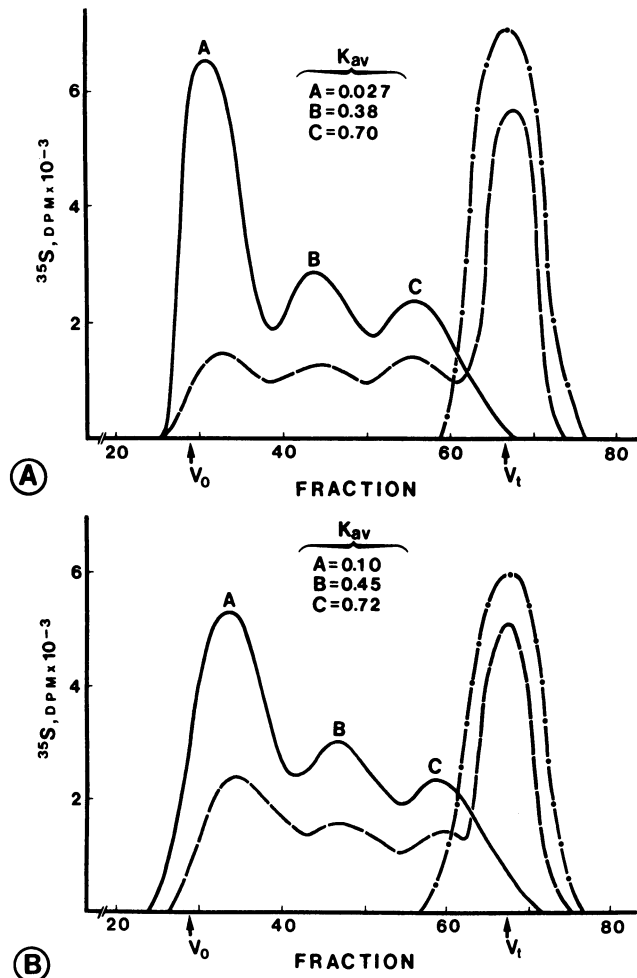


Figure 10. Sepharose CL-4B chromatograms of [<sup>35</sup>S]-sulfate-labeled PGs extracted from (A) day 1 control and (B) 7-d mannose-exposed embryonic kidneys, before (—) and after treatments with heparitinase (---) alone or successively with heparitinase and chondroitinase-ABC (-●-). In the mannose group, radioactivity is decreased in the various peaks and all the peaks have shifted to relatively higher  $K_{av}$  values.

ical studies indicate that both the processes were accompanied by significant changes in the metabolism of PGs.

Mannose induced in metanephric explants a generalized decrease in the de novo synthesis of PGs and alterations in their biochemical characteristics. The PGs synthesized on day 7 were of slightly smaller size (increased  $K_{av}$  value), which may be due to a reduction or delay in the transfer of sugar chains onto the PG core peptide in that GAG chains were of similar size in both the control and experimental groups. Xyloside is the only agent that has been shown to interfere with the addition of the glycosaminoglycan chains to the serine residues of PG core protein (39); whether mannose specifically has a similar effect remains to be determined. In mannose-exposed metanephric explants, after [<sup>35</sup>S]-sulfate labeling, fewer grains were seen over the Golgi complexes compared to control by autoradiography and de novo synthesized PGs had a decreased charge density suggesting a post-translational defect in sulfotransferase activity and/or sulfation of GAGs at the level of the Golgi complex. A similar defect has been demonstrated in streptozotocin-induced diabetes (40), which together with this study,

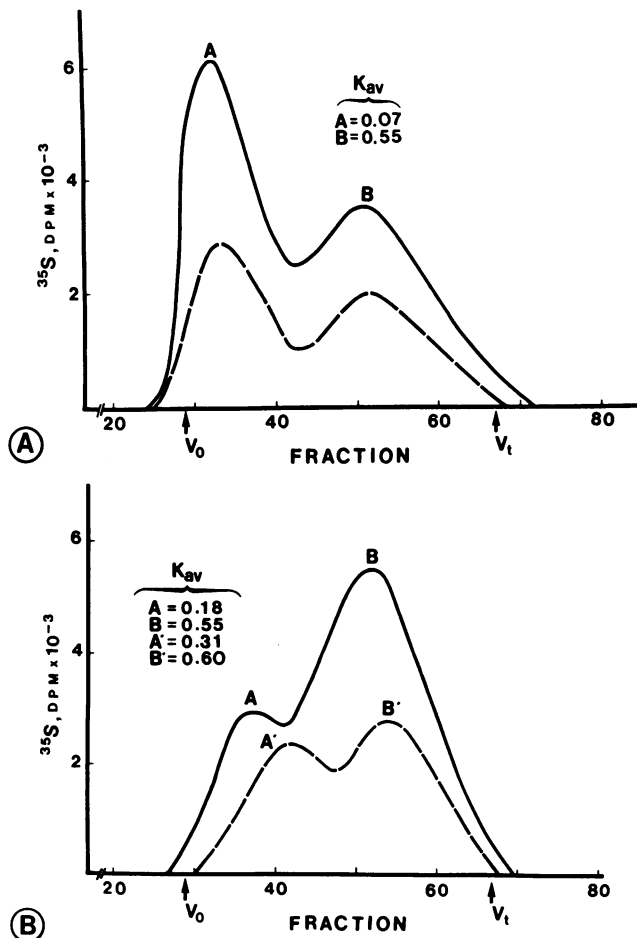


Figure 11. Sepharose CL-4B chromatograms of [<sup>35</sup>S]labeled PGs in the media fraction on day (A) 1 and (B) 7 of metanephric culture. (A) On day 1, the elution profiles of control (—) and mannose-exposed (---) kidneys are similar except for decreased radioactivity in the peaks of mannose group. (B) On day 7, the  $K_{av}$  values for both peaks in the mannose group (---) have shifted to a higher value compared to the control (—), indicating the synthesis of relatively lower molecular weight PGs.

suggests that the impairment in sulfation of GAGs may be related to hyperglycemia. Mannose induced an increase in the proportion in the CS-PG vs. HS-PG with time in the metanephric kidney which may possibly be due to a relative increase in mesenchymal vs. epithelial cells. It has been shown that HS-PG is synthesized mainly by the glomerular epithelial cells and CS-PG by the mesenchymal and mesangial cells (41–43). Thus, mannose induced inhibition of glomerulogenesis could result in a greater proportion of mesenchymal vs. epithelial cells and thereby a proportionate greater de novo synthesis of CS-PG vs. HS-PG. There is also the possibility that at the post-translational level of the Golgi system that mannose induced an increase of synthesis of CS-PG relative to HS-PG.

Although the PG synthesis was dramatically reduced after mannose exposure, the total protein synthesis, as determined by [<sup>35</sup>S]methionine labeling, was minimally affected. Immunoprecipitation of other labeled extracellular matrix proteins, i.e., type IV collagen and laminin revealed only slight reductions in their de novo synthesis (Fig. 13). This indicates that hyperglycemic levels of mannose selectively perturbs the biosynthesis of core peptides of PGs. The mechanism for this selective effect is

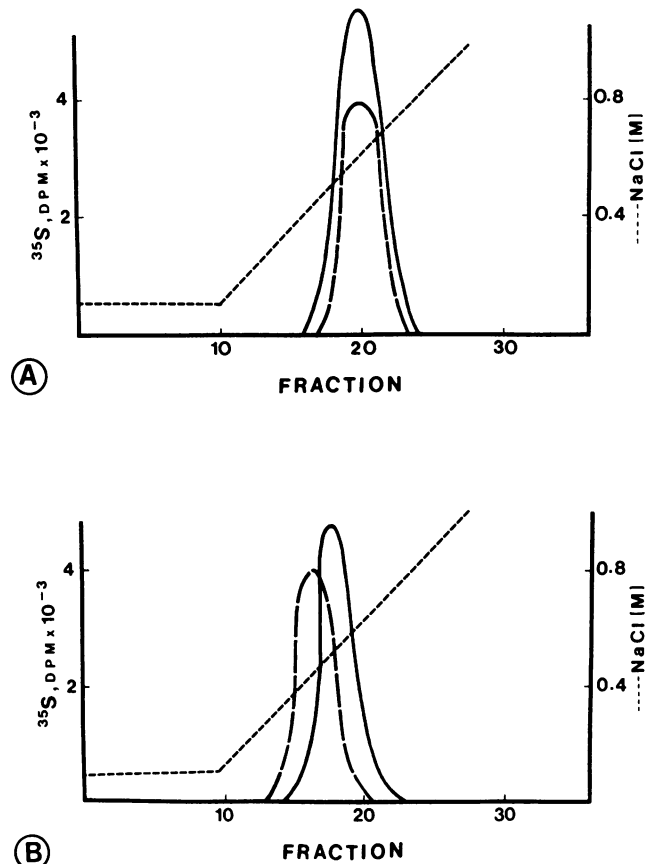


Figure 12. DEAE-Sepharose chromatograms of [<sup>35</sup>S]labeled PGs in the media fraction on day (A) 1 and (B) 7 of metanephric culture. (A) On day 1, the elution profiles of control (—) and mannose-exposed (---) kidneys are similar except for decreased radioactivity in the peaks of mannose group. (B) On day 7, the PGs of the mannose group (---) eluted at a relatively lower salt concentration as compared to the control (—), indicating the synthesis of PGs with lower charge density characteristics.

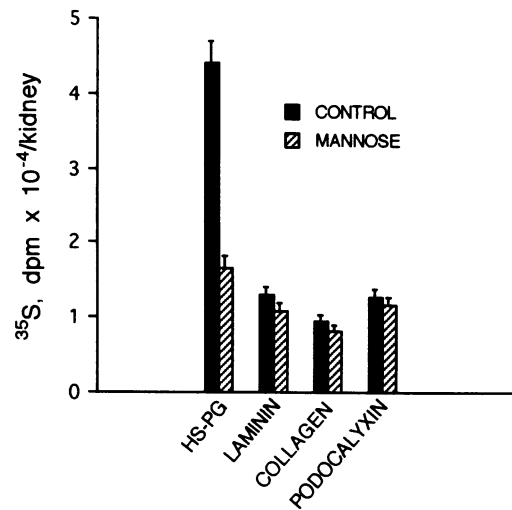
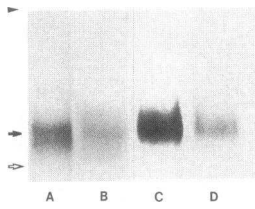


Figure 13. Radioactivity per kidney of [<sup>35</sup>S]methionine-labeled glycoproteins immunoprecipitated by specific antibodies after 4 d of exposure to mannose. Incorporated radioactivity immunoprecipitated by anti-HS-PG antibody is greatly reduced while only minor decreases occurred in radioactivity immunoprecipitated by other antibodies ( $n = 25$ ).



**Figure 14.** Autoradiograms of SDS-polyacrylamide-agarose gel electrophoretograms revealing comigration of [<sup>35</sup>S]methionine-labeled and immunoprecipitated PGs (lanes A and B) and [<sup>35</sup>S]sulfate-labeled non-immunoprecipitated PGs (lanes C and D). The samples in lanes A and B are from the control and mannose-exposed kidneys, respectively. Samples in lanes C and D are from control kidneys except that the sample in lane D was digested with heparitinase before electrophoresis. The arrowhead represents the point of application; the white arrow indicates the migration of cartilage specific chondroitin sulfate-proteoglycan ( $M_r \sim 2.6 \times 10^6$ ).

unknown but may be related to the relatively fast turnover of PGs as compared with other matrix proteins. Hyperosmotic levels of mannose did not affect the integral biosynthetic functions of the glomerular cells because the de novo synthesis of other proteins was not significantly altered. Moreover, hyperosmotic mannitol at concentrations similar to mannose had no adverse effect on the biosynthesis of PGs.

Several findings suggest that mannose retarded cell differentiation in metanephric explants: in glomerular cells the nuclear/cytoplasmic ratio was increased and nuclei were prominently enlarged, common features in dedifferentiated cells (44); and the structural maturation of epithelial foot processes was significantly arrested and they had a dramatic reduction in reactivity with *Helix pomatia* lectin, which is specific for D-GalNAc residues at the base of the epithelial foot processes (Figs. 4 D and 7) (45, 46). Thus, the effect of elevated levels of mannose on cell differentiation and on the synthesis of PGs which modulate organogenesis suggests that hyperglycemia impaired organogenesis.

Mechanisms by which the mannose perturbs the biosynthesis of PGs and expression of epithelial foot process-specific gly-

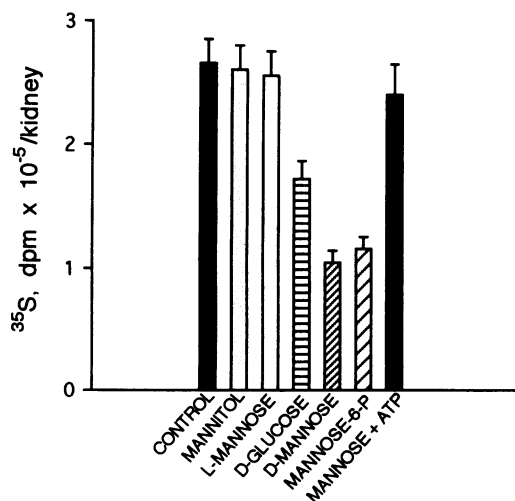


**Figure 15.** [<sup>35</sup>S]sulfate incorporation per metanephric kidney in the presence of mannitol, L-mannose, D-glucose, D-mannose, mannose 6-phosphate, and mannose + 0.1 mM ATP. Mannitol and L-mannose did not decrease incorporation of [<sup>35</sup>S]sulfate. D-Glucose reduced the sulfate incorporation but to a lesser degree as compared to D-mannose. Mannose 6-phosphate greatly decreased incorporation similar to mannose. Supplementation of D-mannose with ATP restored the radioincorporation to ~ 90% of control levels ( $n = 25$ ).

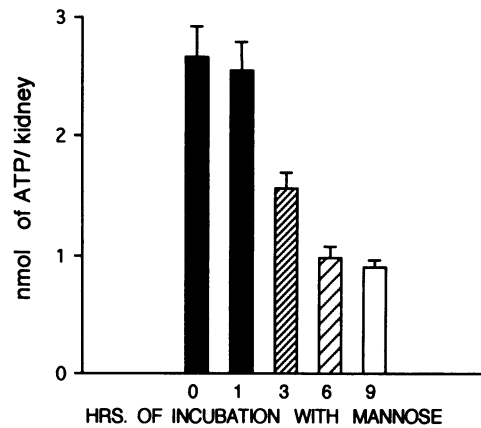


**Figure 16.** Effect of mannose (10 mg/ml) on the cellular ATP levels as a function of time ( $n = 25$ ).

coproteins are unknown. Mannose may impair DNA-replication inasmuch as the de novo pyrimidine synthesis is inhibited in diabetic states (9). This is unlikely in our model in that mannose did not significantly alter total [<sup>3</sup>H]thymidine incorporation. A second possibility is that the conversion of mannose into mannose 6-phosphate may inhibit the transport of PGs from the intracellular to the extracellular compartment. With mannose exposure, labeling of sulfated glycoproteins was decreased only in the extracellular compartment of metanephric kidney suggesting a defect in cellular transport of the de novo synthesized PGs to the extracellular compartment. In human fibroblasts, mannose 6-phosphate blocks the transport of pericellular PGs into the extracellular compartment, perhaps via receptor-mediated mechanisms (47). Our experiments with mannose 6-phosphate yielded results similar to those for mannose and thus support, in part, a defect in the cellular transport of PGs. Thirdly, mannose may affect morphogenesis by competing with mannose 6-phosphate for its receptor. A number of biologically active peptides, including proliferin (48) and transforming growth factor  $\beta$  (49) contain mannose-6-phosphate, and their interactions with the mannose 6-phosphate receptor may be necessary to maintain growth and differentiation. However, our experiments indicate that the concomi-

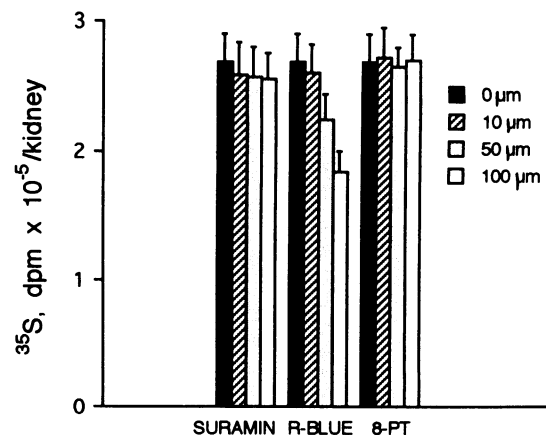


**Figure 17.** Effect of various concentrations of purinoceptor antagonists, i.e., suramin, reactive blue-2 (*R-blue*) and 8-phenyltheophylline (*8-PT*) on the [<sup>35</sup>S]sulfate incorporation in the presence of mannose (10 mg/ml) and ATP (100 μM) in the medium ( $n = 25$ ).

tant exposure of metanephric kidneys to mannose and mannose 6-phosphate did not further alter de novo synthesis of PGs or DNA replication.

Another possibility for the perturbation in the metabolism of PGs may be due to the depletion of cellular ATP induced by mannose. Mannose is initially converted by nonspecific hexokinase to mannose 6-phosphate, and subsequently isomerized into fructose 6-phosphate which is further phosphorylated to fructose 1,6-diphosphate. These steps consume large amounts of ATP and cause depletion of metabolic fuel which is necessary for the glycolytic and other biosynthetic pathways. Our findings indicate that inclusion of mannose in the medium indeed causes remarkable depletion of intracellular ATP. The depletion of ATP may account for the decreased de novo synthesis of PGs because in our hands supplementing the medium of mannose-exposed metanephric kidneys with 100  $\mu$ M of ATP resulted in the restoration of their biosynthesis. The mechanism by which ATP restores the synthesis of PGs may either be related to the repletion of its cellular stores directly, or by initially binding to the cell surface purinoceptors and thereafter modulating various intracellular events, e.g., rise in cAMP levels (50). The fact that reactive blue-2, one of the P<sub>2</sub> purinoceptor antagonist, partially (~ 30%) inhibited the ATP-induced recovery of de novo synthesis of PGs suggests that its effect, at least in part, is receptor-mediated. Lastly, 8-phenylthephylline (P<sub>1</sub> receptor antagonist) did not significantly alter the synthesis of PGs, thereby suggesting that the hydrolyzed product of ATP, such as adenosine may not be involved in the ATP-induced restoration processes discussed above.

In summary, D-mannose causes the depletion of cellular ATP and induces remarkable alterations in the biosynthesis of PGs, and above all perturbs the morphogenesis/organogenesis of metanephric kidney.

## Acknowledgments

This study was supported by National Institutes of Health grants DK-28492 and DK-42304.

## References

1. Pederson, L. M., I. Tygstrup, and J. Pederson. 1964. Congenital malformations in newborn infants of diabetic women: correlations with maternal diabetic vascular complications. *Lancet*. i:1124-1126.
2. Comess, L. J., P. H. Bennett, T. A. Burch, and M. Miller. 1969. Congenital anomalies and diabetes in the Pima Indians of Arizona. *Diabetes*. 18:471-477.
3. Soler, N. G., C. H. Walsh, and J. M. Malines. 1976. Congenital malformations in infants of diabetic mothers. *Q. J. Med.* 45:303-313.
4. Fuhrmann, K., H. Reihar, K. Semmler, F. Fisher, M. Fischer, and E. Glockner. 1983. Prevention of congenital malformations in infants of insulin-dependent diabetic mothers. *Diabetes Care*. 6:219-224.
5. Watanabe, G., and T. H. Ingalls. 1973. Congenital malformations in the offspring of alloxan diabetic mice. *Diabetes*. 12:66-67.
6. Deuchar, E. M. 1977. Embryonic malformations in rats, resulting from maternal diabetes: preliminary observations. *J. Embryol. Exp. Morphol.* 41:93-99.
7. Eriksson, U. J., N. J. Lewis, and N. Freinkel. 1983. Growth retardation during early organogenesis in embryos of experimentally diabetic rats. *Diabetes*. 33:281-284.
8. Freinkel, N., N. J. Lewis, S. Akazawa, S. I. Roth, and L. Gorman. 1984. The honey bee syndrome: implications of the teratogenicity of mannose in rat embryo culture. *N. Engl. J. Med.* 110:223-230.
9. Buchanan, T. A., and N. Freinkel. 1988. Fuel-mediated teratogenesis: symmetric growth retardation in the rat fetus at term after a circumscribed exposure to D-mannose during organogenesis. *Am. J. Obstet. Gynecol.* 158:663-669.
10. Thiery, J. P., J. L. Duband, U. Rutishauser, and G. M. Edelman. 1982. Cell adhesion molecules in early chicken embryogenesis. *Proc. Natl. Acad. Sci. USA*. 79:6737-6741.
11. Vestweber, D., R. Kemler, and P. Ekblom. 1985. Cell-adhesion molecule uvomorulin during kidney development. *Dev. Biol.* 112:213-221.
12. Duband, J. L., T. Volberg, I. Sabanay, J. P. Thiery, and B. Geiger. 1988. Spatial and temporal distribution of the adherens-junction-associated adhesion molecule A-CAM during avian embryogenesis. *Development*. 103:325-344.
13. Hay, E. D. 1983. Collagen and embryonic development. *In Cell Biology of the Extracellular Matrix*. E. D. Hay, editor. Plenum Press, New York. 381-389.
14. Toole, B. P. 1983. Glycosaminoglycans in morphogenesis. *In Cell Biology of the Extracellular Matrix*. E. D. Hay, editor. Plenum Press, New York. 259-288.
15. Brenner, B. M. 1990. Determinants of epithelial differentiation during early nephrogenesis. *J. Am. Soc. Nephrol.* 1:127-139.
16. Banerjee, S. D., R. H. Cohn, and M. R. Bernfield. 1977. Basal lamina of embryonic salivary epithelium and role in maintaining epithelial morphogenesis. *J. Cell Biol.* 73:445-463.
17. Silverstein, G. B., and C. W. Daniel. 1982. Glycosaminoglycans in the basal lamina and extracellular matrix of the developing mouse mammary duct. *Dev. Biol.* 90:215-222.
18. Smith, C. I., S. Robert-Hilfer, R. L. Searls, M. A. Nathanson, and M. D. Allodol. 1990. Effects of B-D-xyloside on differentiation of the respiratory epithelium in the fetal mouse lung. *Dev. Biol.* 138:45-52.
19. Lelongt, B., H. Makino, and Y. S. Kanwar. 1987. Maturation of the developing renal glomerulus with respect to basement membrane proteoglycans. *Kidney Int.* 32:498-506.
20. Lelongt, B., H. Makino, T. M. Dalecki, and Y. S. Kanwar. 1988. Role of proteoglycans in renal development. *Dev. Biol.* 128:256-276.
21. Liu, Z. Z., T. M. Dalecki, N. Kashihara, E. Wallner, and Y. S. Kanwar. 1991. Effect of puromycin on metanephric differentiation: morphologic, autoradiographic and biochemical studies. *Kidney Int.* 39:1140-1155.
22. Platt, J. L., D. M. Brown, K. Granlund, and T. R. Oegema, and D. J. Klein. 1987. Proteoglycan metabolism associated with mouse metanephric development: morphological and biochemical effect of beta-D-xyloside. *Dev. Biol.* 123:293-306.
23. Kanwar, Y. S., L. J. Rosenzweig, A. Linker, and M. L. Jakubowski. 1983. Decreased de novo synthesis of glomerular proteoglycans in diabetes: biochemical and autoradiographic evidence. *Proc. Natl. Acad. Sci. USA*. 80:2275-2279.
24. Cohen, M. P. 1987. Biochemical aspects of diabetic nephropathy. *In Renal Basement Membranes in Health and Disease*. B. G. Hudson and R. G. Price, editors. Academic Press, Inc., New York. 255-272.
25. Avner, E. D., D. Ellis, T. Temple, and R. Jaffe. 1982. Metanephric development in serum free organ culture. *In Vitro (Rockville)*. 18:675-682.
26. Makino, H., J. T. Gibbons, M. K. Reddy, and Y. S. Kanwar. 1986. Nephritogenicity of antibodies to proteoglycans of the glomerular basement membranes-I. *J. Clin. Invest.* 77:142-156.
27. Dixit, S. N. 1985. Isolation, purification and characterization of intact and pepsin-derived fragments of laminin from human placenta. *Connect. Tissue Res.* 14:31-40.
28. Ozaki, I., Y. Ito, A. Fukatsu, N. Suzuki, F. Yoshida, Y. Watanabe, N. Sakamoto, and S. Matsuo. 1990. A plasma membrane antigen of rat glomerular epithelial cells. *Lab. Invest.* 63:707-716.
29. Salpeter, M. M., and L. Bachman. 1972. Autoradiography. *In Principles and Techniques in Electron Microscopy: Biological Applications*. M. A. Hayat, editor. Van Nostrand Reinhold, New York. 221-278.
30. Weibel, E. R. 1972. The value of stereology in analyzing structure and function of cells and organs. *J. Microsc.* 95:3-13.
31. Wasteson, A. 1971. A method for determination of molecular weight and molecular weight distribution of chondroitin sulfate. *J. Chromatogr.* 59:87-97.
32. Kanwar, Y. S., V. C. Hascall, and M. L. Jakubowski. 1984. Effect of beta-D-xyloside on glomerular proteoglycans. I. Biochemical studies. *J. Cell Biol.* 99:715-722.
33. Lang, G. P., and G. Michael. 1974. D-Glucose-6-phosphate and D-fructose-6-phosphate. *In Methods of Enzymatic Analysis*. H. V. Bergmeyer, editor. Verlag Chemie GmbH, Weinheim, FRG. 1238-1242.
34. Nakazawa, K., K. Fujimori, A. Takana, and K. Inoue. 1990. Reversible and selective antagonism by suramin of ATP-activated inward current in PC12 pheochromocytoma cells. *Br. J. Pharmacol.* 101:224-226.
35. Burnstock, G. 1990. Classification and characterization of purinoceptors. *In Purines in Cellular Signaling: Targets for New Drugs*. K. A. Jacobson, J. W. Daly, and V. Manganiello, editors. Springer-Verlag, Inc., New York. 241-253.
36. Smeaton, T. C., and B. D. Eichner. 1983. Measurement of DNA with an automatic spectrophotometer. *Anal. Biochem.* 131:394-396.
37. Reeves, W. H., J. P. Caulfield, and M. G. Farquhar. 1978. Differentiation of epithelial foot processes and filtration slits: sequential appearance of occluding junctions, epithelial polyanion and slit membranes in developing glomeruli. *Lab. Invest.* 39:90-100.
38. Bernstein, J., F. Cheng, and J. Roszka. 1981. Glomerular differentiation in metanephric culture. *Lab. Invest.* 45:183-190.
39. Lohmander, L. S., V. C. Hascall, and A. I. Kaplan. 1979. Effect of 4-methylumbelliferyl-B-D xylopyranoside on chondrogenesis and proteoglycan synthesis in chick limb bud mesenchymal cultures. *J. Biol. Chem.* 254:10,551-10,561.

40. Kjellen, L., D. Bielefeld, and M. Hook. 1983. Reduced sulfation of liver heparan sulfate in experimentally diabetic rats. *Diabetes*. 32:337-342.
41. Striker, G. E., M. A. Lange, K. Mackay, K. Bernstein, and L. J. Striker. 1987. Glomerular cells in vitro. *Adv. Nephrol.* 16:169-186.
42. Kanwar, Y. S., L. J. Rosenzweig, and M. L. Jakubowski. 1983. Distribution of de novo synthesized sulfated glycosaminoglycans in the glomerular basement membrane and mesangial matrix. *Lab. Invest.* 49:216-225.
43. Yaoita, E., K. Oguri, E. Okayama, K. Kawasaki, S. Kobayashi, I. Kihara, and M. Okayama. 1990. Isolation and characterization of proteoglycans synthesized by cultured mesangial cells. *J. Biol. Chem.* 265:522-531.
44. Cotran, R. S., V. Kumar, and S. L. Robbins. 1989. Neoplasia. In Robbins Pathologic Basis of Disease. W. B. Saunders Co., Philadelphia. 239-305.
45. Roth, J., D. Brown, and L. Orci. 1983. Regional distribution of *N*-acetyl-D-galactosamine residues in the glycocalyx of glomerular podocytes. *J. Cell Biol.* 96:1189-1196.
46. Kunz, A., D. Brown, J. D. Vassalli, M. Konturri, T. Kumpulainen, and L. Orci. 1985. Ultrastructural localization of glycocalyx domains in human kidney podocytes using the lectin-gold technique. *Lab. Invest.* 53:413-420.
47. Roff, C. F., R. W. Wozniak, J. Blenis, and J. L. Wang. 1983. The effect of mannose 6-phosphate on the turn over of cell surface glycosaminoglycans. *Exp. Cell Res.* 144:334-344.
48. Lee, S. J., and D. Nathans. 1988. Proliferin secreted by cultured cells binds to mannose 6-phosphate receptors. *J. Biol. Chem.* 263:3521-3527.
49. Purchio, A. F., J. A. Cooper, A. M. Brunner, M. N. Lioubin, L. E. Gentry, K. S. Kovacina, R. A. Roth, and H. Marquardt. 1988. Identification of mannose 6-phosphate in two asparagine-linked sugar chains of recombinant transforming growth factor- $\beta$ 1. *J. Biol. Chem.* 263:14211-14215.
50. Kim, K. T., M. Diverse-pierluissi, W. N. Kopell, and E. W. Westhead. 1990. ATP effects on secretion and second messenger production in bovine chromaffin cells. *Ann. N. Y. Acad. Sci.* 603:435-436.